ARTICLE

ACS chemical biology

N^{η}-Substituted Arginyl Peptide Inhibitors of Protein Arginine *N*-Methyltransferases

Ted M. Lakowski[†,∥], Peter 't Hart[‡,∥], Christopher A. Ahern[§], Nathaniel I. Martin[‡,*], and Adam Frankel[†,*]

[†]Faculty of Pharmaceutical Sciences, The University of British Columbia, Vancouver, British Columbia, Canada, [‡]Department of Medicinal Chemistry & Chemical Biology, University of Utrecht, Utrecht, The Netherlands, and [§]Department of Anaesthesiology, The University of British Columbia, Vancouver, British Columbia, Canada, [∥]These authors contributed equally to this work.

ABSTRACT Protein arginine *N*-methyltransferases (PRMTs) catalyze the post-translational methylation of arginine residues within substrate proteins. Their roles in the epigenetic regulation of gene expression make them viable targets for drug discovery. Peptides containing a single arginine residue substituted at the guanidino nitrogen (N^{η}) with an ethyl group bearing zero to three fluorine atoms (R1-1, -2, -3, and -4) have been synthesized and tested for methylation and inhibition activity with PRMT1, PRMT6, and CARM1. Only the nonfluorinated R1-1 peptide is methylated by PRMT1, demonstrating that the N^{η}-substituted arginine is accommodated by its active site. The R1-1 ethyl-substituted guanidine N^{η} was further identified as the methylation site *via* mass spectrometry. Although weak inhibitors of CARM1, R1-1, -2, -3, and -4 are potent inhibitors of PRMT1 and PRMT6. These peptides are more potent against PRMT1 than product inhibitor peptides, showing that N^{η}-substituted arginyl peptides do not work by a purely product inhibitor mechanism. A trend of increasing potency with an increase in the number of fluorine atoms is observed for PRMT1, which may result from the corresponding change in the guanidino dipole moment. Modeling of the ethyl-arginine moiety of the R1-1 peptide demonstrates that the active site of PRMT1 accommodates such modifications. N^{η}-Substituted arginyl peptides represent lead compounds for the further development of inhibitors that target the methyl-acceptor binding site of PRMTs.

Protein arginine *N*-methyltransferases (PRMTs) are a family of conserved enzymes that catalyze the post-translational methylation of arginine residues within substrate proteins. PRMTs transfer methyl groups from the co-substrate *S*-adenosyl-L-methionine (AdoMet) to arginine residues within substrate proteins, forming the products *S*-adenosyl-L-homocysteine (AdoHcy) and *N*-methylated arginine residues. Two methyl groups can be transferred to each arginine residue, producing N^{η}-monomethyl-arginine (MMA) and asymmetric $N^{\eta 1}$,$N^{\eta 1}$-dimethyl-arginine (aDMA) or symmetric $N^{\eta 1}$,$N^{\eta 2}$-dimethyl-arginine (sDMA). (For the purpose of clarity the IUPAC convention of nomenclature for L-arginine and its derivatives is used.) PRMTs that produce aDMA or sDMA are called type I or type II enzymes, respectively (*1*).

PRMTs methylate RNA- and DNA-binding proteins such as small nuclear or heterogeneous nuclear ribonucleoproteins (snRNPs or hnRNPs) and histones. Through this activity, PRMTs influence RNA metabolism (*e.g.*, transcription and splicing) and act as transcriptional co-repressors or co-activators (*1*). Along with lysine methylation, acetylation, and ubiquitination and serine phosphorylation, arginine methylation is an epigenetic histone modification that regulates gene expression as part of the histone code (*2*). PRMTs appear to play roles in cancer and viral replication (*3*–*6*), as well as cardiovascular disease (*7*). In addition to the recent success of histone deacetylase inhibitors in treating cancer, the emerging role of PRMTs in disease suggests that these enzymes are viable targets for drug discovery (*8*).

PRMTs catalyze methylation(s) at the guanidino nitrogen N^{η} of specific arginine residues in target proteins. Mechanistically, PRMTs position the incoming nucleophilic N^{η} for attack at the AdoMet methyl group, lead-

*Corresponding authors, n.i.martin@uu.nl, afrankel@interchange.ubc.ca.

Received for review June 4, 2010 and accepted August 11, 2010.

Published online August 11, 2010

10.1021/cb100161u

ing to N^{η}-methylation and production of the byproduct AdoHcy (*9*). While transition state analogues are often pursued in the drug discovery process, the most potent PRMT inhibitors described to date tend to target the AdoMet binding site common to most methyltransferases and display little PRMT selectivity (*8*). Recent screening efforts have, however, uncovered new classes of small molecules that display apparent selective inhibition of PRMTs while retaining potency (*10*–*12*). The symmetric urea compound arginine methyltransferase inhibitor 1 (AMI-1) was the first PRMT inhibitor identified in this fashion (*10*). By molecular docking AMI-1 was shown to span both the AdoMet and substrate arginine binding sites (*13*), whereas it did not inhibit UV cross-linking of AdoMet to PRMT1 (suggesting that it does not compete for the AdoMet binding site) (*10*). The related compound AMI-5 did reduce UV cross-linking and by molecular docking was found to bind exclusively to the AdoMet binding site (*10, 13*). The suramin-like sulfonated ureas, to which AMI-1 is related, bind to multiple proteins. To mitigate this issue, carboxy analogues of AMI-1 were designed that are nearly as potent as the parent compound while retaining PRMT selectivity (*14*). Identified in a virtual library screen, the thioglycolic amide RM65 has been shown to inhibit PRMT1 and cause histone hypomethylation in HepG2 cells (*12*). Molecular docking suggests that this compound binds to the AdoMet binding site. Most recently, bisubstrate PRMT inhibitors have been described that combine AdoMet and the guanidine group of arginine *via* a variable linker to produce selective inhibition of PRMT1 (*15*).

Rather than targeting the AdoMet binding site common to many methyltransferases, a more rational strategy for production of a PRMT-specific inhibitor is to target the substrate arginine-binding site. Potential inhibitors made this way could provide an intrinsic selectivity for PRMTs over other methyltransferases. Using a recently developed methodology (*16*), a series of 12-mer peptides based on a consensus sequence for methylation in the PRMT substrate fibrillarin were prepared, each containing a single arginine residue substituted on the guanidino N^{η} with an ethyl group bearing an increasing number of fluorine atoms (Figure 1). These peptides are here designated R1-1, -2, -3, and -4 and are based upon the previously described R1 series of peptides (*i.e.*, R1, R1(MMA), R1(aDMA), and R1(sDMA)) (*17*). Here we examine R1-1, -2, -3, and -4 for PRMT methylation and inhibition activity with PRMT1, PRMT6, and CARM1. Only R1-1 is methylated by PRMT1. Using mass spectrometry (MS) the ethyl-substituted N^{η} of R1-1 is identified as the site of methylation, producing $N^{\eta 1}$-methyl-$N^{\eta 1}$-ethyl-arginine (methyl-Et-Arg). The PRMT1 active site can therefore accommodate both N^{η}-ethyl-arginine (Et-Arg) and AdoMet simultaneously. Since fluoroethyl substituents are isosteric with the ethyl substituent, R1-2, -3, and -4 are also thought to bind to the active site of PRMT1. Inhibition studies with all four peptides using a MS assay show strong inhibition of PRMT1 and PRMT6 and weak inhibition of CARM1. A trend of increasing potency with the addition of fluorine atoms is observed for PRMT1 that may be explained by the corresponding change in the guanidino dipole moment. A model, based upon an existing structure of PRMT1, depicts how Et-Arg of R1-1 can fit into its active site.

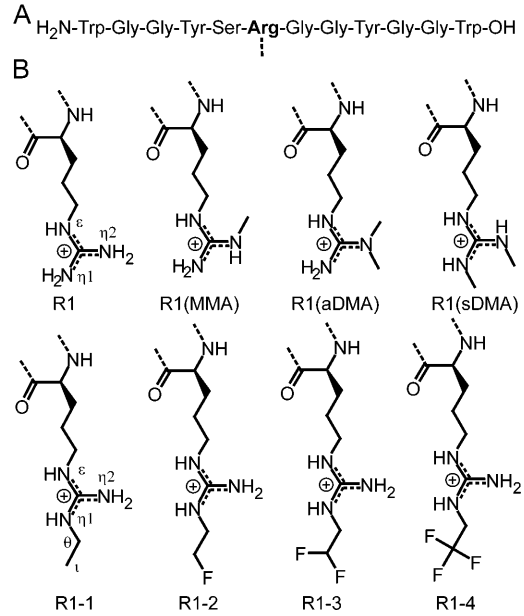

Figure 1. Substituted arginine peptides. A) The parent R1 peptide sequence. B) Structures of the N^{η}-substituted arginine residue within the R1 peptide.

RESULTS AND DISCUSSION

Methylation of N^{η}-Substituted Arginyl Peptides. The similarity of R1-1, -2, -3, and -4 to R1 and R1(MMA) (Figure 1) suggested that they might be PRMT substrates as well as inhibitors. We tested the propensity of PRMT1, PRMT6, and CARM1 to methylate R1-1, -2, -3, and -4 by incubation with [methyl-^{14}C]AdoMet, followed by separation *via* tricine gel electrophoresis, and detection us-

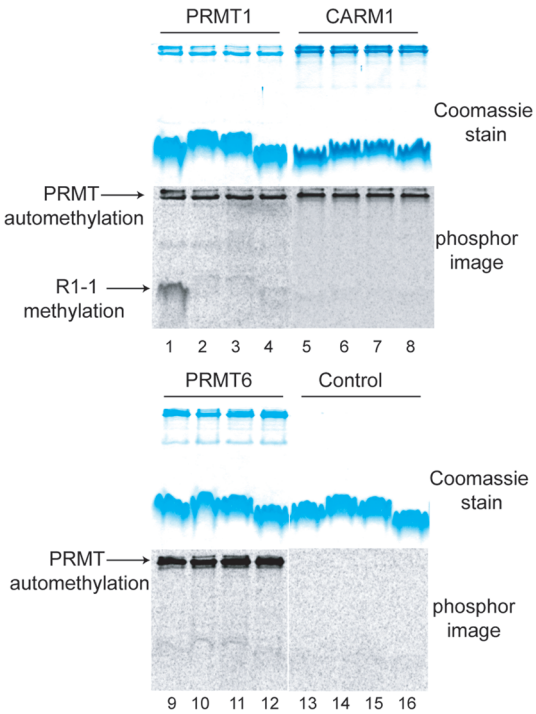

Figure 2. Methylation of N^{η}-substituted arginyl peptides. Methylation of R1-1, -2, -3, and -4 peptides by PRMT1 (lanes 1−4), CARM1 (lanes 5−8), and PRMT6 (lanes 9−12) and no-enzyme controls (lanes 13−16). Coomassie blue stain is depicted on top, and the corresponding phosphor image is on the bottom. PRMT automethylation and the methylation of R1-1 by PRMT1 (lane 1) are indicated. Phosphor images are brightness- and contrast-enhanced for visualization.

ing storage phosphor screens (Figure 2). In addition to the expected automethylation signal, we also observed a methylation signal only from the R1-1 peptide when incubated with PRMT1. No other above-background methylation signals are observed for other combinations tested, including no-enzyme controls. These results indicate that the Et-Arg moiety fits into the active site of PRMT1 and is methylated. To confirm that methylation is enzyme-dependent, R1-1 was incubated with [methyl-^{14}C]AdoMet along with increasing concentrations of PRMT1. Figure 3, panel A shows increasing methylation activity of R1-1 with increasing PRMT1.

To determine the site of methylation on R1-1, the peptide was incubated with and without PRMT1 in the presence of either AdoMet or [methyl-^{14}C]AdoMet. The acid-hydrolyzed reactions were separated by UPLC and assessed with tandem MS, scanning for the parent ions 203, 217, and 219 *m*/*z* (Figure 3, panel B), corresponding, respectively, to Et-Arg, methyl-Et-Arg, and ^{14}C-methyl-Et-Arg. Detection of a peak in the no-enzyme reaction at 3.24 min confirms that a mass corresponding to Et-Arg survives the hydrolysis procedure. A peak at ~4.7 min in the AdoMet with PRMT1 reaction (Figure 3, panel B, middle) has the mass of a singly methylated Et-Arg. A peak with a similar retention in the [methyl-^{14}C]AdoMet with PRMT1 reaction (Figure 3, panel B, bottom) has the mass of ^{14}C-methyl-Et-Arg. No peaks are detected at masses corresponding to dimethylated Et-Arg (data not shown), ruling out the possibility of multiple methyl transfers. The fragment ion spectra from the chromatograms in Figure 3, panel B are shown in Figure 3, panel C for the no-enzyme control (top), AdoMet with PRMT1 (middle), and [methyl-^{14}C]AdoMet with PRMT1 (bottom) reactions. The no-enzyme reaction exhibits a similar fragmentation pattern to that observed with aDMA, including the presence of a peak at 46 *m*/*z* that has been previously determined to be dimethylammonium (*18*). In this case the peak represents its isomer, ethylammonium (Figure 3, panel C, top). Only two peaks at 70 and 116 *m*/*z* in the reaction with AdoMet and PRMT1 are also found in the no-enzyme control. Therefore, all other peaks represent fragments that have been modified by the addition of a methyl group. With this in mind, the structures of fragments derived from the reaction with AdoMet and PRMT1 are also readily determined (Figure 3, panel C, middle). These structures are further confirmed when [methyl-^{14}C]AdoMet is used (Figure 3, panel, C bottom) wherein all methylated fragments are 2 amu higher, owing to the difference in isotope mass. These data demonstrate that R1-1 is methylated once on the N^{η}-ethyl-substituted nitrogen atom.

The observation that R1-1 is methylated suggests that the PRMT1 active site can simultaneously accommodate Et-Arg in the substrate arginine binding site and AdoMet in its binding site. Moreover, the presence of the N^{η}-ethyl substitution does not eliminate methyl transfer but rather restricts it to the N^{η}-ethyl-substituted nitrogen atom as fragment ions resulting from methylation on the other guanidino nitrogens are not detected. No methylation activity is observed against R1-2, -3, or -4, and no 217 and 219 *m*/*z* peaks are detected in the no-enzyme control reactions (data not shown). Also, consistent with the results illustrated in Figure 2, methylation is not detected with CARM1 or PRMT6 (data not

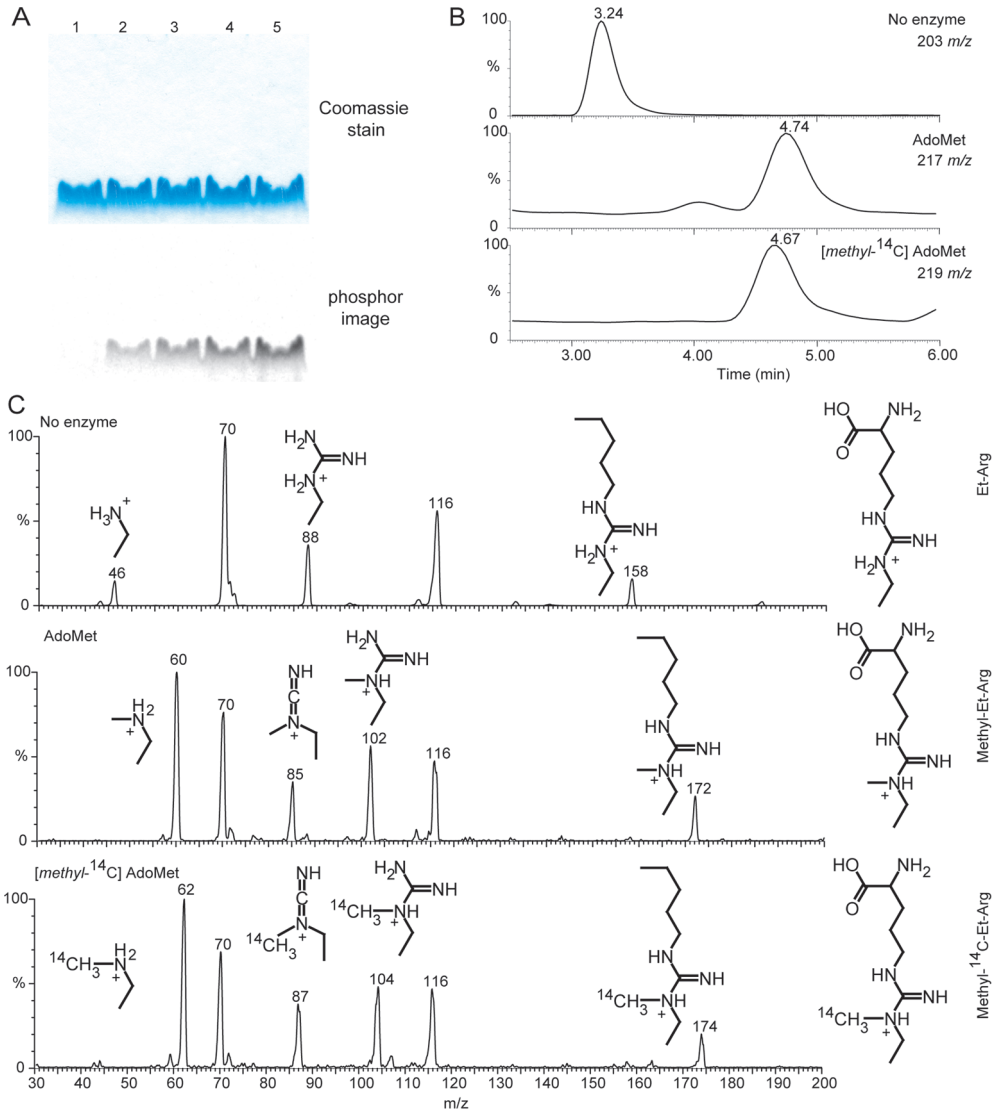

Figure 3. Formation of methylated R1-1 by PRMT1. A) The methylation of R1-1 with 0, 2.0, 4.0, 5.9, and 11.7 μM PRMT1 incubated with constant R1-1 and [methyl-^{14}C]AdoMet, and separated by tricine gel electrophoresis. B) Separation of Et-Arg from hydrolyzed R1-1 UPLC-MS recording ion 203 *m/z* (top) and methylated Et-Arg from hydrolyzed methylation reactions with AdoMet using recording ion 217 *m/z* (middle) or with [methyl-^{14}C]AdoMet using recording ion 219 *m/z* (bottom). C) Corresponding fragment ion scans from chromatograms in panel B. The proposed structure is displayed on the right of the spectra and the fragments are above or to the left of the associated peaks.

shown). Since the fluoroethyl substituents of R1-2, -3, and -4 are isosteric with the ethyl substituent of R1-1, they likely fit into the active sit of PRMT1 as well. The lack of methylation activity against these N^{η}-fluoroethyl-substituted peptides may be due to the electron-withdrawing effects of the fluorine atoms, indicating that R1-2, -3, and -4 may act as PRMT inhibitors.

Having determined that R1-1 is methylated by PRMT1, we compared the enzymatic activity of PRMT1 against R1-1 to the parent peptides R1 and R1(MMA).

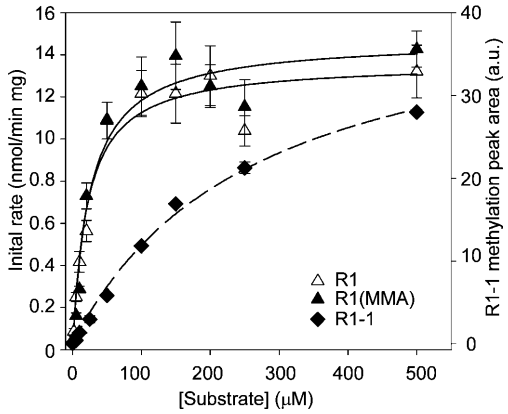

Figure 4. Comparison of methylation of R1 and R1(MMA) to R1-1. The initial rate of methylation of R1 (△) and R1(MMA) (▲) by PRMT1 as measured by the accumulation of MMA and aDMA in hydrolyzed methylation reactions. Each point represents the mean and standard deviation of two measurements. The K_M values for R1 and R1(MMA) are 24.4 ± 2.6 and 24.8 ± 2.6 μM, respectively. The initial rate of formation of methylated R1-1 is determined by measuring the peak area of methyl-Et-Arg from hydrolyzed reactions of PRMT1 with R1-1 (◆) (dashed line with the scale on the right). The K_M for R1-1 is 263 ± 4.0 μM.

The initial rate of methylation of R1 and R1(MMA) by PRMT1, as measured by the accumulation of MMA and aDMA in hydrolyzed methylation reactions, is displayed in Figure 4. The K_M values for R1 and R1(MMA), derived by fitting the activity data to the Michaelis−Menten−Henri equation, are 24.4 ± 2.6 and 24.8 ± 2.6 μM, respectively. Despite the absence of a methyl-Et-Arg standard, it was possible to measure the activity of PRMT1 against R1-1 using the peak area generated by an UPLC-MS/MS assay that detects the diagnostic peaks listed in Figure 3, panel C (middle). The methylation of R1-1 by PRMT1, as measured by the accumulation of methyl-Et-Arg in hydrolyzed methylation reactions, is displayed in Figure 4. The K_M value, derived by fitting the data as described above, is 263 ± 4.0 μM. If K_M is taken as a surrogate for the dissociation constant, then R1-1 has a 10-fold lower affinity for PRMT1 than either R1 or R1(MMA). An alternate explanation is that although R1-1 can bind to the enzyme, catalysis is slow in comparison to R1 and R1(MMA). Such an interpretation, further supported by the IC_{50} data presented below, suggests that steric hindrance by the ethyl group on N^{η} might decrease the rate of catalysis and that R1-1 may be more accurately described as an inhibitor of PRMT1.

TABLE 1. Inhibition constants for PRMT1, PRMT6, and CARM1

PRMT1			
Inhibitor	IC_{50} (μM)[a]	Inhibitor	IC_{50} (μM)[b]
R1-1	29.0 ± 25	R1-1	56.5 ± 22
R1-2	19.2 ± 6.1	R1-2	39.4 ± 7.8
R1-3	17.0 ± 4.5	R1-3	28.5 ± 10
R1-4	13.9 ± 1.8	R1-4	27.5 ± 1.2
R1(aDMA)	74.4 ± 10		
R1(sDMA)	350 ± 210		

CARM1		PRMT6	
Inhibitor	IC_{50} (μM)[b]	Inhibitor	IC_{50} (μM)[b]
R1-1	179 ± 0.9	R1-1	4.82 ± 3.3
R1-2	260 ± 13	R1-2	14.2 ± 2.6
R1-3	254 ± 6.4	R1-3	13.9 ± 0.7
R1-4	168 ± 19	R1-4	9.43 ± 1.4

[a]AdoHcy production was measured. [b]MMA and aDMA production was measured.

Inhibition of PRMT by N^{η}-Substituted Arginyl Peptides. To test the hypothesis that R1-1, -2, -3, and -4 are PRMT inhibitors, their IC_{50} values were determined and compared to IC_{50} values for product inhibitors R1(aDMA) and R1(sDMA) (Figure 1) by measuring formation of the byproduct AdoHcy (Figure 5, panel A). R1-1, -2, -3, and -4 all appear to be inhibitors of PRMT1, and the resulting IC_{50} values are listed in Table 1. The proposed inhibitory mechanism of these peptides could be considered similar to the product inhibition that results from the formation of aDMA-containing products by PRMTs (*17*). However, Figure 5, panel A and Table 1 show that R1-1, -2, -3, and -4 are more potent inhibitors of PRMT1 than R1(aDMA) or R1(sDMA). The former peptides exhibit as much as a 5-fold greater inhibitory potency than R1(aDMA) and 24-fold greater inhibitory potency than R1(sDMA). Importantly, the assay to detect AdoHcy is used in this case because the addition of product inhibitors R1(aDMA) and R1(sDMA) would obfuscate *de novo* methylarginine formation in the reaction, rendering enzyme activity determination impossible using assays that detect N^{η}-methylarginines (MMA and aDMA).

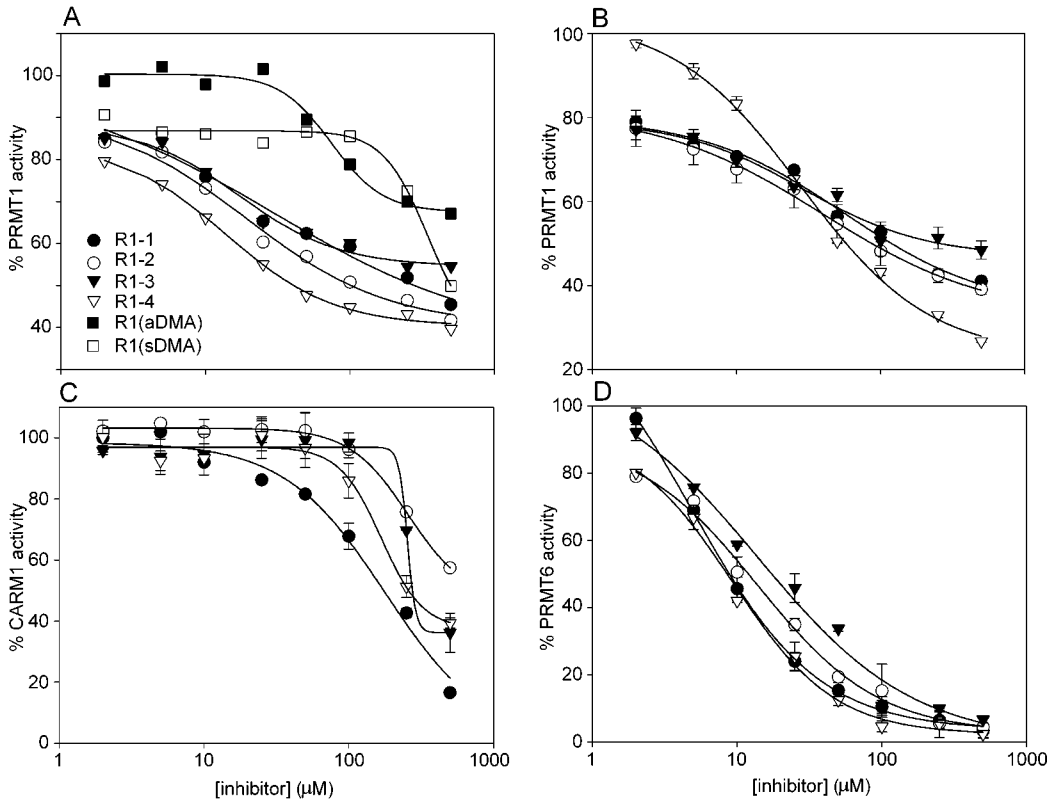

Figure 5. Inhibition of PRMT1, CARM1, and PRMT6. A) The inhibition of PRMT1 by R1-1 (●), R1-2 (○), R1-3 (▼), R1-4 (▽), R1(aDMA) (■), and R1(sDMA) (□) as measured by the decrease in AdoHcy formation. The inhibition of PRMT1 (B), CARM1 (C), or PRMT6 (D) by R1-1 (●), R1-2 (○), R1-3 (▼), and R1-4 (▽) as measured by the decrease in methylarginine formation. Each point represents the mean and standard deviation of two measurements.

Although PRMT1 activity drops off precipitously, the maximal inhibition by R1-2, -3, and -4 is 55−38% of enzyme activity. The remaining activity may be caused by PRMT automethylation, which could obscure the potency of candidate inhibitors. To remove the signal generated by automethylation in subsequent IC_{50} studies, the PRMT enzyme was removed by passage through centrifugal filters with molecular weight cut-offs sufficient to allow retention of the enzyme and complete passage of the substrate through the filter after the reaction was stopped (Supplementary Figure S1). The filtrate, containing substrate and products free of enzyme, were hydrolyzed, and the activity was measured by detection of N^{η}-methylarginines. The results of these IC_{50} studies for PRMT1 are displayed in Figure 5, panel B and Table 1. Measuring N^{η}-methylarginine formation after removal of the automethylation products results in higher IC_{50} values. Although the maximal effect of inhibition improved for R1-4 compared to the AdoHcy assay, (Figure 5, panels A and B), R1-1, R1-2, and R1-3 still produced a maximal 40−50% reduction in enzyme activity. It is unclear why this may be the case, but it is interesting to note that the structure of PRMT1 has been shown to contain several accessory binding grooves distal to the active site (*19*), which may bind to peptide inhibitors and result in decreased inhibitory potency. However, we were unable to prepare reactions with very high inhibitor concentrations because of their low solubility beyond 500 μM. The inhibition data for CARM1 and PRMT6 by R1-1, -2, -3, and -4 using the same assay to detect N^{η}-methylarginine formation are displayed in Figure 5, panels C and D, respectively, and the IC_{50} values are listed in Table 1. The IC_{50} values for these peptides against CARM1 are 3- to 9-fold higher than the corresponding values for PRMT1 and 18- to 37-fold higher than for PRMT6. Significant inhibition of CARM1

is not observed at concentrations below 250 μM, suggesting that relative to PRMT1 and PRMT6, R1-1, -2, -3, and -4 are poor inhibitors of CARM1. The IC_{50} values for these peptides against PRMT6 are 3- to 12-fold lower than for PRMT1, and concentrations from 250 to 500 μM result in as much as a 97% reduction in PRMT6 activity. Thus, R1-1, -2, -3, and -4 are slightly more selective for PRMT6 than PRMT1.

Structural studies have revealed the presence of acidic grooves for substrate binding on PRMT1 (*19*), underscoring the importance of peptide sequence for targeting substrates or inhibitors to PRMT active sites. Accordingly, R1 and R1(MMA) are substrates for PRMT1 (Figure 4), PRMT6 (*17*), and CARM1 (Supplementary Figure S2). Therefore, the low inhibitory potency of R1-1, -2, -3, and -4 for CARM1 relative to PRMT1 and PRMT6 cannot be readily explained by the inability of the peptide portion of these inhibitors to bind to CARM1. Moreover, the PRMT6 K_M values for R1 and R1(MMA) are 20- and 8-fold (*17*) higher than the corresponding K_M values for PRMT1, yet PRMT6 has lower IC_{50} values for R1-1, -2, -3, and -4. These results suggest that while important for targeting the N^{η}-substituted arginines to PRMT active sites, the peptide portion on its own cannot predict inhibitory potency.

The bisubstrate enzyme mechanism that PRMT6 and presumably all PRMTs use is ordered sequentially, where the co-substrate AdoMet binds first and the co-product AdoHcy dissociates last (*17*). This mechanism is supported by structural investigations of CARM1, which show that AdoMet binding occurs first, resulting in a conformational change that forms the binding site for protein substrates (*20, 21*). The IC_{50} values and the maximal reduction in PRMT activity are dependent upon the concentrations of AdoMet and protein substrate. Ideally, the concentrations of each substrate should be at their respective apparent K_M values. Under these conditions the IC_{50} value derived from inhibition assays will be at least 2 times its inhibitor dissociation constant (K_I) (*22*). Importantly, maintaining the substrate concentrations at or near the apparent K_M values provides a baseline by which different enzymes can be compared because PRMTs exhibit dissimilar affinities for AdoMet (Thomas *et al.*, accepted manuscript) and often use different substrates with varying K_M values (*17, 23*). Using the same substrate concentration for multiple enzymes can produce disparate IC_{50} values that result from K_M differences for enzymes and substrates rather than any intrinsic property of the inhibitor (*22*).

For comparison, an IC_{50} study similar to that displayed in Figure 5, panel B was performed with PRMT1 and the potent product inhibitor AdoHcy (Supplementary Figure S3). The resulting IC_{50} of 6.94 ± 1.6 μM for AdoHcy is 4-fold more potent than the best PRMT1 inhibitors (R1-3 and R1-4) but in the same range as values for R1-1, -2, -3, and -4 against PRMT6.

Properties of N^{η}-Substituted Arginines. An examination of PRMT1 inhibition (Table 1) reveals a trend of decreasing IC_{50} values with an increasing number of fluorine atoms on the N^{η}-ethyl substituent. This trend is observed with assays detecting AdoHcy and N^{η}-methylarginines (Figure 5, panels A and B). Physicochemical parameters of the arginine guanidino group change upon fluorination, including partial charges and dipole moment. These altered parameters may contribute to the decreasing trend of IC_{50} values with increasing fluorine atom substitution. Figure 6, panel A depicts the calculated dipole moments and partial charges for the various substituted arginines employed in this study. Although the partial charges of the guanidino N^{η} do not change appreciably, the C^{ι} of the ethyl substituent increases from −0.343 to 1.271 electrons upon trifluorination. (Gaussian09 reports atomic partial charges in units of electrons.)

A concomitant change in dipole moment is observed in the substituted guanidino groups upon fluorination (Figure 6, panel B). The directions of the guanidino dipole moments for MMA, aDMA, sDMA, and Et-Arg do not vary significantly from that of arginine, yet dramatic differences in the direction of dipole moment are observed with increasing fluorine atom substitution, resulting in a near reversal (up to 154°) in the direction of the dipole moment (Figure 6, panel B). This alteration in polarity may affect the hydrogen bonding that normally occurs between PRMT and arginine substrate. In particular, the conserved residue Glu153 of PRMT1 may be impacted (*19*). Glu153 is believed to play a critical role in catalysis by redistributing the positive charge toward the $N^{\eta 2}$ of the guanidino group of arginine, leaving the lone pair of electrons of $N^{\eta 1}$ free to attack the methyl group of AdoMet (*9*). This charge redistribution may also help to prevent electrostatic repulsion between the AdoMet sulfonium and the arginine guanidino group (Figure 7, panel A). The change in dipole moment (Gaussian09 orientates the arrow of the dipole moment toward the positive end of the dipole) observed with fluoroethyl-substituted R1-2, -3, and -4 progressively redistributes the positive charge of the guanidino group to $N^{\eta 1}$ or N^{ε}, thereby preventing catalysis. As the PRMT1 Glu153Gln

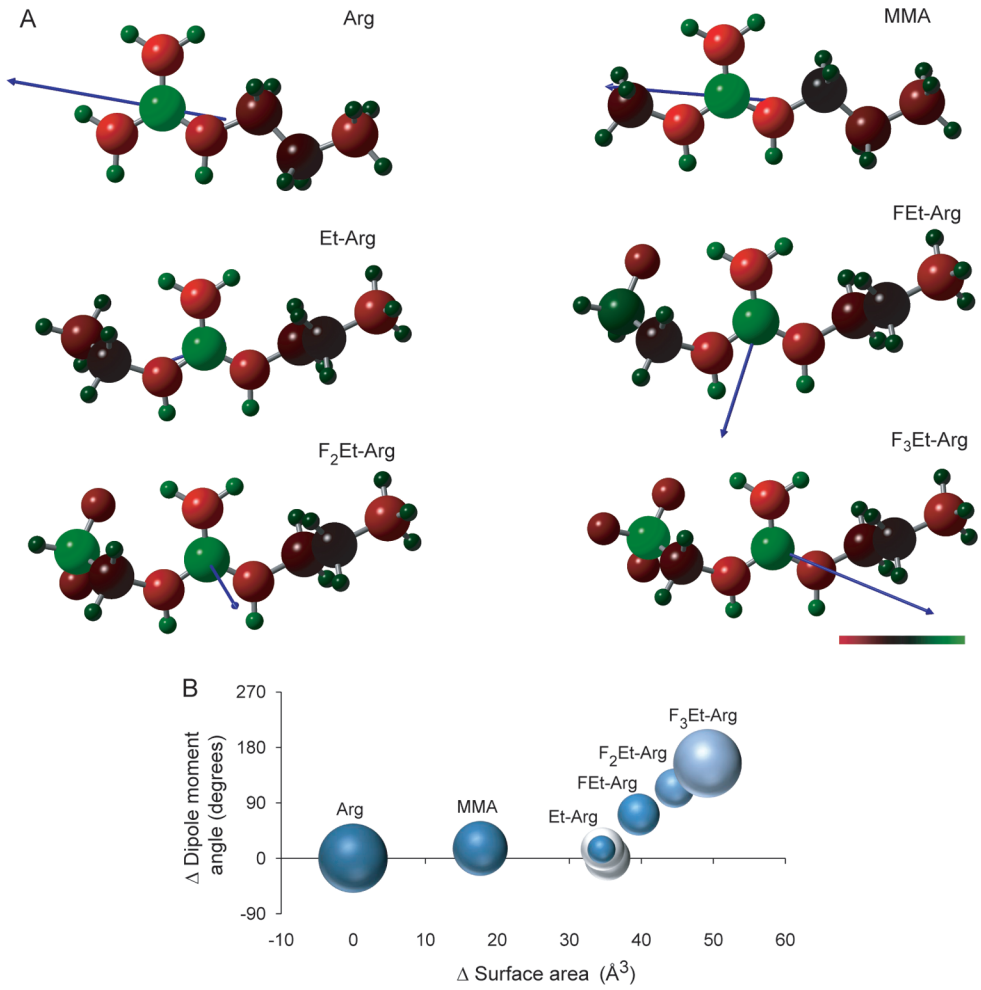

Figure 6. Physicochemical properties of N^{η}-substituted arginines. A) Gaussian09/GaussView 5.0 generated gas phase HF/6-31G structures of the Arg side chain and its derivatives starting at C^{β} to eliminate side chain interactions with amino and carboxylate groups during energy minimization. The scale bar indicates atomic partial charges ranging from −1.0 (red) to +1.0 (green) electrons, and the blue arrow indicates the magnitude and direction of the dipole moment. B) Changes to surface area and direction of dipole moment relative to the Arg side chain are plotted. The dipole moment magnitude for each structure corresponds to the diameter of each data bubble (where Arg is 5.64 D). Data for aDMA and sDMA are shown in white for comparison.

mutant is not active (presumably because it cannot redistribute the positive charge to $N^{\eta 2}$) (*19*), it follows that substituents that redistribute the positive charge of the guanidino to $N^{\eta 1}$ or N^{ε} may also result in no methylation activity. The ethyl substitution on R1-1 does not alter the direction of the guanidino dipole moment and likely does not interrupt ionic interaction with Glu153 of PRMT1. These differences likely account for why R1-1 is methylated by PRMT1 whereas R1-2, -3, and -4 are not.

Changes to dipole moments of substituted guanidino groups have proven important in structure−activity relationships (SAR) of other compounds. For example, analogues of cimetidine have an optimal dipole moment angle, which in turn helps to maximize hydrogen-bonding interactions with its target receptor to improve its H2 antagonist activity (*24*).

The ethyl group addition to the arginine side chain results in a nearly 24% increase in total volume, which is

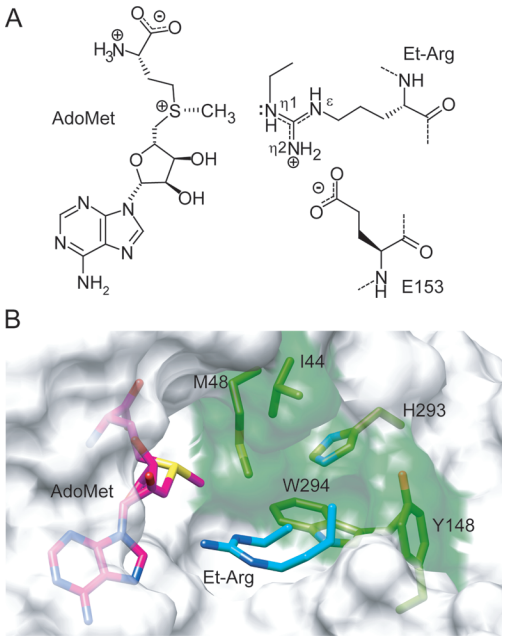

Figure 7. Proposed structure of Et-Arg in the active site of PRMT1. A) Proposed schematic of the active site of PRMT1 showing the redistribution of the positive charge of the substrate Et-Arg guanidino group to the $N^{\eta 2}$, leaving the lone pair of electrons on $N^{\eta 1}$ free to attack the methyl group of AdoMet. B) The active site transparent surface of PRMT1 with AdoHcy (magenta) and the target arginine residue (cyan) (PDB 1OR8). An ethyl group is added to the arginine structure to mimic the potential binding of R1-1. Residues in close proximity to the N^{η}-substituted guanidine group are highlighted in green. A methyl group is added to the sulfur atom of AdoHcy to mimic the structure of AdoMet. The structure is rendered using Chimera (*31*). Please note that I44 is missing C^{δ} according to PDB 1OR8.

the same volume increase found for aDMA and sDMA (Figure 6, panel B). Consistent with the generally accepted notion that fluorine is an isosteric replacement for hydrogen, only a modest 9% increase in total volume from Et-Arg to F_3Et-Arg side chains was calculated. Although subtle, it is plausible that these changes in substituent size can account for observed potency differences.

Fit of N^{η}-Substituted Arginyl Peptides into the PRMT1 Active Site. R1-1, -2, -3, and -4 inhibit PRMT1 and PRMT6, and R1-1 is a weak substrate for PRMT1. Given the nearly equivalent molecular volumes of Et-Arg and the product inhibitor aDMA (Figure 6, panel B), it seems reasonable that both residues can fit into the active site of PRMT1. To examine the fit of substituted arginines within the active site of PRMT1, we used an existing crystal structure of PRMT1 with a peptide substrate and AdoHcy (occupying the AdoMet binding site) (*19*). Shown in Figure 7, panel B is the enzyme−substrate complex in which an ethyl group has been added to the guanidino $N^{\eta 1}$ of the substrate arginine residue, chosen on the basis of the mechanism delineated in a previous structural study (*9*). A methyl group was also added to the AdoHcy sulfur atom to mimic the structure of AdoMet. The model shows that the PRMT1 active site can accommodate Et-Arg and suggests how a methyl group can be added to the ethylated $N^{\eta 1}$. In addition, when a structure of CARM1 is superimposed onto the structure of PRMT1 described above (data not shown), there is a relatively good fit between the structures (rmsd = 0.9 Å). PRMT1 contains a contiguous surface of residues conserved among PRMTs that form a hydrophobic pocket on one side of the active site in which the ethyl substituent resides (Figure 7, panel B). Residues I44 in PRMT1 and V56 in PRMT6 (analogous residue *via* sequence alignment) are replaced by the one nonconserved residue Q159 in CARM1, although this position is distal to the ethyl substituent and may not play a role in the observed selectivity.

Conclusion. IC_{50} values derived under different conditions using different assays are not comparable (*22*). However, the similarity between the IC_{50} values for R1-1, -2, -3, and -4 and the potent product inhibitor AdoHcy suggest that substituted peptides are relatively potent against PRMT6 and to a lesser extent PRMT1. The recent development of irreversible chloroacetamidine inhibitors is an additional illustration of how peptides represent an excellent starting point for exploring PRMT-selective inhibition (*25*). In the present study a 12-mer peptide scaffold is employed as a vehicle for the N^{η}-substituted arginine residue. Future work may involve other chemical modifications and substitutions to N^{η}, as well as attempts to minimize or mimic the peptidic motif given the poor drug-like properties of peptides.

The success of histone deacetylase inhibitors in the treatment of cancer suggests that targeting the epigenetic regulation of gene expression is a feasible strategy (*8, 26*). Arginine methylation is one of many

forms of this regulation that has not been investigated thoroughly for its pharmaceutical potential. The evidence presented in this study suggests that N^{η}-substituted arginyl peptides are promising leads to be further developed into future classes of PRMT-selective inhibitors.

METHODS

PRMT Genes Expression and Purification. The pET28a (Novagen) plasmids harboring human PRMT6 and PRMT1 have been described previously (*17*). The gene for human CARM1 was amplified from the pTracer EF/V5 plasmid (a gift from Dr. Mark Bedford, The University of Texas M. D. Anderson Cancer Center) using the primers 5′-GGA ATT CCA TAT GGC AGC GGC GGC GGC GGC-3′ and 5′-GGA ATT CCT AGC TCC CGT AGT GCA TGG TGT TGG TCG GG-3′ and subcloned into pET28a using the *Nde*I and *Eco*RI restriction sites. Histidine-tagged human PRMT1, CARM1, and PRMT6 were expressed and purified according to previously described methods (Thomas *et al.*, accepted manuscript). All PRMT enzymes were quantified by densitometry as described previously (*23*). The synthesis, purification, and quantitation of the histone H3 and histone H4 tail peptides as well as the peptides R1, R1(MMA), R1(aDMA), and R1(sDMA) have been described previously (*17, 23*).

Synthesis of N^{η}-Substituted Arginyl Peptides. The R1-1, -2, -3, and -4 series of N^{η}-substituted peptides were prepared following standard Fmoc SPPS protocols. The required N^{η}-modified L-arginine building blocks were prepared from a common thiourea precursor as previously described (see Supporting Information for details) (*16*). Peptides were assembled on the 2-chlorotrityl resin working at 0.25 mmol scale. With the exception of the N^{η}-modified L-arginine building blocks, peptide couplings were performed using 4.0 equiv of protected Fmoc amino acid, 4.0 equiv of BOP reagent, and 8.0 equiv of DIPEA in a total volume of 10 mL of DMF at RT for 1 h. Alternatively, incorporation of the N^{η}-modified L-arginine building residues was performed using 2.0 equiv of the N^{η}-modified L-arginine building blocks, 2.0 equiv of BOP reagent, and 4.0 equiv of DIPEA in a total volume of 10 mL of DMF at RT overnight. Peptide couplings were verified using the Kaiser and bromophenol blue tests. Upon completion of SPPS, peptides were cleaved from the resin and deprotected using a mixture of 95:2.5:2.5 TFA/TIS/H_2O followed by Et_2O precipitation to yield the crude peptides. Each peptide was purified to homogeneity using RP-HPLC, employing a Prosphere C18 column (250 × 22 mm, 300 Å, 10 μm) with a gradient of 5→95% acetonitrile (0.1% TFA) in 90 min at a flow rate of 11.5 mL min^{-1}. Peptide identity was confirmed by MALDI-MS analysis, in each case providing the expected mass (see Supporting Information for RP-HPLC traces and MALDI mass spectra).

Methylation of N^{η}-Ethylated R1 Peptides. PRMT1, CARM1, or PRMT6 at 2.0 μM were incubated with 400 μM R1-1, -2, -3, or -4 and 190 μM [methyl-^{14}C]AdoMet (Amersham (2.06 GBq $mmol^{-1}$)) in methylation buffer (50 mM HEPES-KOH (pH 8.0), 10 mM NaCl, and 1.0 mM dithiothreitol (DTT)) at 37 °C for 16 h. Samples were mixed with sample dilution buffer and separated using tricine gel electrophoresis (*27*). Gels were fixed (*28*), stained with Coomassie blue, dried, and exposed to storage phosphor screens (GE Healthcare). To show enzyme-dependent methylation, similar reactions were carried out on R1-1 with 0 to 11.7 μM PRMT1.

Position of Methylation of R1-1. Two groups of reactions were prepared. The first group contained 100 μM AdoMet, and the second group contained 100 μM [methyl-^{14}C]AdoMet. Each group consisted of three 40-μL reactions: (1) 4.0 μM PRMT, (2) 400 μM R1-1, and (3) 4.0 μM PRMT with 400 μM R1-1. Reactions were incubated for 16 h, dried in a vacuum centrifuge, and hydrolyzed in the vapor phase with 6 M HCl for 24 h at 110 °C. The dried hydrolysate was reconstituted in 100 mM HCl, and basic amino acids were purified using Oasis MCX SPE columns (Waters) (*29*). Extracted amino acids were reconstituted in 0.1% formic acid and 0.05% TFA and analyzed *via* UPLC-MS/MS on a Quatro Premier XE electrospray mass spectrometer (Micromass MS Technologies). Fragment ions were recorded with a 30-V cone voltage and a 20-eV collision energy. For the AdoMet group the parent ions 203, 217, and 231 *m*/*z* were selected, corresponding to Et-Arg, methyl-Et-Arg, and dimethyl-Et-Arg, respectively. The [methyl-^{14}C]AdoMet group was analyzed similarly except that the parent ions were 203, 219, and 235 *m*/*z*.

The apparent K_M of R1-1 for PRMT1 was measured using 0 to 500 μM R1-1 with 2.0 μM PRMT1 with a constant 250 μM AdoMet for 1 h. The reactions were processed as in the proceeding paragraph and analyzed using UPLC-MS/MS multiple reaction monitoring for the parent ion 217 *m*/*z* (corresponding to methyl-Et-Arg) and the associated diagnostic fragment ions 60, 85, 102, and 172 *m*/*z* with a 30-V cone voltage and a 20-eV collision energy.

Determination of Apparent K_M Values. In order to compare IC_{50} values obtained from different bisubstrate enzyme reactions, inhibition experiments were performed at or near the K_M values for both substrates (*22*). The AdoMet K_M values for PRMT1 and PRMT6 have been measured previously (*17, 23*). The apparent K_M values for PRMT1 with the histone H4 peptide and for PRMT6 with the histone H3 peptide were measured previously (Thomas *et al.*, accepted manuscript). The CARM1 apparent K_M for AdoMet and H3 tail were measured using a previously described MS assay (*23*). Briefly, CARM1 at 800 nM was incubated with 100 μM H3 tail peptide and from 0.5 to 200 μM AdoMet or with constant 200 μM AdoMet and from 1.0 to 200 μM H3 tail. The data for both sets of CARM1 reactions were fit to the Michaelis−Menten−Henri equation using SigmaPlot (SYSTAT), with resulting K_M values for AdoMet and H3 tail of 15.6 ± 1.8 and 13.2 ± 2.9 μM, respectively (Supplementary Figure S4).

Inhibition Studies. Inhibition studies were performed with 0 to 500 μM and R1-1, -2, -3, or -4 and 200 nM PRMT1, PRMT6, or 400 nM CARM1 in a 80-μL reaction volume. For PRMT1, the H4 tail and AdoMet concentrations were 15 and 10 μM, respectively. For CARM1, the H3 tail and AdoMet concentrations were both 20 μM. For PRMT6, the H3 tail and AdoMet concentrations were 5.0 and 20 μM, respectively. PRMT1 and PRMT6 were incubated for 1 h and CARM1 was incubated for 2 h. Reactions were stopped by flash freezing, thawed in ice, and filtered through prechilled Microcon Ultracel YM-30 centrifugal filters in a prechilled centrifuge, and the filtrate was dried in a vacuum centrifuge. Samples were hydrolyzed, and methylated arginines were assayed (*23*). Identical inhibition studies were performed as described above for PRMT1, but with the addition of the product inhibitors R1(aDMA) and R1(sDMA) for comparison. These reactions were assayed using a method that detects the co-product AdoHcy (*30*).

Acknowledgment: We thank Andras Szeitz, the manager of the MS facility in the Faculty of Pharmaceutical Sciences at The University of British Columbia. This work was supported by the Canadian Institutes of Health Research Grant 79271 and the Canada Research Chairs program (to A.F.), the Dutch Science

Foundation (NWO-VENI grant to N.I.M.), as well as the Canadian Institutes of Health Research Grant 56858, the Heart and Stroke Foundation of Canada, and the Michael Smith Foundation for Health Research (to C.A.A.).

Supporting Information Available: This material is available free of charge *via* the Internet at http://pubs.acs.org.

REFERENCES

1. Bedford, M. T., and Clarke, S. G. (2009) Protein arginine methylation in mammals: who, what, and why, *Mol. Cell 33*, 1–13.
2. Strahl, B. D., and Allis, C. D. (2000) The language of covalent histone modifications, *Nature 403*, 41–45.
3. Frietze, S., Lupien, M., Silver, P. A., and Brown, M. (2008) CARM1 regulates estrogen-stimulated breast cancer growth through up-regulation of E2F1, *Cancer Res. 68*, 301–306.
4. Michaud-Levesque, J., and Richard, S. (2009) Thrombospondin-1 is a transcriptional repression target of PRMT6, *J. Biol. Chem. 284*, 21338–21346.
5. Xie, B., Invernizzi, C. F., Richard, S., and Wainberg, M. A. (2007) Arginine methylation of the human immunodeficiency virus type 1 Tat protein by PRMT6 negatively affects Tat Interactions with both cyclin T1 and the Tat transactivation region, *J. Virol. 81*, 4226–4234.
6. Yoshimatsu, M., Toyokawa, G., Hayami, S., Unoki, M., Tsunoda, T., Field, H. I., Kelly, J. D., Neal, D. E., Maehara, Y., Ponder, B. A., Nakamura, Y., Hamamoto, R. (2010) Dysregulation of PRMT1 and PRMT6, type I arginine methyltransferases, is involved in various types of human cancers, *Int. J. Cancer.* DOI: 10.1002/ijc.25366.
7. Teerlink, T., Luo, Z., Palm, F., and Wilcox, C. S. (2009) Cellular ADMA: Regulation and action, *Pharmacol. Res. 60*, 448–460.
8. Copeland, R. A., Solomon, M. E., and Richon, V. M. (2009) Protein methyltransferases as a target class for drug discovery, *Nat. Rev. Drug Discovery 8*, 724–732.
9. Zhang, X., Zhou, L., and Cheng, X. (2000) Crystal structure of the conserved core of protein arginine methyltransferase PRMT3, *EMBO J. 19*, 3509–3519.
10. Cheng, D., Yadav, N., King, R. W., Swanson, M. S., Weinstein, E. J., and Bedford, M. T. (2004) Small molecule regulators of protein arginine methyltransferases, *J. Biol. Chem. 279*, 23892–23899.
11. Spannhoff, A., Heinke, R., Bauer, I., Trojer, P., Metzger, E., Gust, R., Schule, R., Brosch, G., Sippl, W., and Jung, M. (2007) Target-based approach to inhibitors of histone arginine methyltransferases, *J. Med. Chem. 50*, 2319–2325.
12. Spannhoff, A., Machmur, R., Heinke, R., Trojer, P., Bauer, I., Brosch, G., Schule, R., Hanefeld, W., Sippl, W., and Jung, M. (2007) A novel arginine methyltransferase inhibitor with cellular activity, *Bioorg. Med. Chem. Lett. 17*, 4150–4153.
13. Ragno, R., Simeoni, S., Castellano, S., Vicidomini, C., Mai, A., Caroli, A., Tramontano, A., Bonaccini, C., Trojer, P., Bauer, I., Brosch, G., and Sbardella, G. (2007) Small molecule inhibitors of histone arginine methyltransferases: homology modeling, molecular docking, binding mode analysis, and biological evaluations, *J. Med. Chem. 50*, 1241–1253.
14. Castellano, S., Milite, C., Ragno, R., Simeoni, S., Mai, A., Limongelli, V., Novellino, E., Bauer, I., Brosch, G., Spannhoff, A., Cheng, D., Bedford, M. T., and Sbardella, G. (2010) Design, synthesis and biological evaluation of carboxy analogues of arginine methyltransferase inhibitor 1 (AMI-1), *ChemMedChem 5*, 398–414.
15. Dowden, J., Hong, W., Parry, R. V., Pike, R. A., and Ward, S. G. (2010) Toward the development of potent and selective bisubstrate inhibitors of protein arginine methyltransferases, *Bioorg. Med. Chem. Lett. 20*, 2103–2105.
16. Martin, N. I., and Liskamp, R. M. (2008) Preparation of N(G)-substituted L-arginine analogues suitable for solid phase peptide synthesis, *J. Org. Chem. 73*, 7849–7851.
17. Lakowski, T. M., and Frankel, A. (2008) A kinetic study of human protein arginine N-methyltransferase 6 reveals a distributive mechanism, *J. Biol. Chem. 283*, 10015–10025.
18. Gehrig, P. M., Hunziker, P. E., Zahariev, S., and Pongor, S. (2004) Fragmentation pathways of N(G)-methylated and unmodified arginine residues in peptides studied by ESI-MS/MS and MALDI-MS, *J. Am. Soc. Mass. Spectrom. 15*, 142–149.
19. Zhang, X., and Cheng, X. (2003) Structure of the predominant protein arginine methyltransferase PRMT1 and analysis of its binding to substrate peptides, *Structure 11*, 509–520.
20. Troffer-Charlier, N., Cura, V., Hassenboehler, P., Moras, D., and Cavarelli, J. (2007) Functional insights from structures of coactivator-associated arginine methyltransferase 1 domains, *EMBO J. 26*, 4391–4401.
21. Yue, W. W., Hassler, M., Roe, S. M., Thompson-Vale, V., and Pearl, L. H. (2007) Insights into histone code syntax from structural and biochemical studies of CARM1 methyltransferase, *EMBO J. 26*, 4402–4412.
22. Yang, J., Copeland, R. A., and Lai, Z. (2009) Defining balanced conditions for inhibitor screening assays that target bisubstrate enzymes, *J. Biomol. Screen. 14*, 111–120.
23. Lakowski, T. M., and Frankel, A. (2009) Kinetic analysis of human protein arginine *N*-methyltransferase 2: Formation of monomethyl- and asymmetric dimethylarginine residues on histone H4, *Biochem. J. 421*, 253–261.
24. Young, R. C., Durant, G. J., Emmett, J. C., Ganellin, C. R., Graham, M. J., Mitchell, R. C., Prain, H. D., and Roantree, M. L. (1986) Dipole moment in relation to H2 receptor histamine antagonist activity for cimetidine analogues, *J. Med. Chem. 29*, 44–49.
25. Obianyo, O., Causey, C. P., Osborne, T. C., Jones, J. E., Lee, Y. H., Stallcup, M. R., and Thompson, P. R. (2010) A chloroacetamidine-based inactivator of protein arginine methyltransferase 1: Design, synthesis, and in vitro and in vivo evaluation, *ChemBioChem 11*, 1219–1223.
26. Bolden, J. E., Peart, M. J., and Johnstone, R. W. (2006) Anticancer activities of histone deacetylase inhibitors, *Nat. Rev. Drug Discovery 5*, 769–784.
27. Schagger, H., and von Jagow, G. (1987) Tricine-sodium dodecyl sulfate-polyacrylamide gel electrophoresis for the separation of proteins in the range from 1 to 100 kDa, *Anal. Biochem. 166*, 368–379.
28. Wiltfang, J., Arold, N., and Neuhoff, V. (1991) A new multiphasic buffer system for sodium dodecyl sulfate-polyacrylamide gel electrophoresis of proteins and peptides with molecular masses 100,000−1000, and their detection with picomolar sensitivity, *Electrophoresis 12*, 352–366.
29. Teerlink, T., Nijveldt, R. J., de Jong, S., and van Leeuwen, P. A. (2002) Determination of arginine, asymmetric dimethylarginine, and symmetric dimethylarginine in human plasma and other biological samples by high-performance liquid chromatography, *Anal. Biochem. 303*, 131–137.
30. Lakowski, T. M., and Frankel, A. (2010) Sources of *S*-adenosyl-L-homocysteine background in measuring protein arginine *N*-methyltransferase activity using tandem mass spectrometry, *Anal. Biochem. 396*, 158–160.
31. Pettersen, E. F., Goddard, T. D., Huang, C. C., Couch, G. S., Greenblatt, D. M., Meng, E. C., and Ferrin, T. E. (2004) UCSF Chimera—a visualization system for exploratory research and analysis, *J. Comput. Chem. 25*, 1605–1612.